PNAS
www.pnas.org

Supplementary Information for

# Nanoanalytical Analysis of Bisphosphonate-Driven Alterations of Microcalcifications using a 3D Hydrogel System and In Vivo Mouse Model

Jessica L. Ruiz[a,b], Joshua D. Hutcheson[c], Luis Cardoso[d], Amirala Bakhshian Nik[c], Alexandra Condado de Abreu[e], Tan Pham[a], Fabrizio Buffolo[a], Sara Busatto[f,g], Stefania Federici[h], Andrea Ridolfi[i,j,k], Masanori Aikawa[a,l], Sergio Bertazzo[e], Paolo Bergese[g,i,m], Sheldon Weinbaum[d,#], Elena Aikawa[a,l,#]

[a] Center for Interdisciplinary Cardiovascular Sciences, Cardiovascular Medicine, Brigham and Women's Hospital, Harvard Medical School, Boston, MA 02115;
[b] Department of Pediatrics, Boston Children's Hospital, Harvard Medical School, Boston, MA 02115;
[c] Department of Biomedical Engineering, Florida International University, Miami, FL 33174;
[d] Department of Biomedical Engineering, City College of New York, New York, NY 10031;
[e] Department of Medical Physics & Biomedical Engineering, University College London, London, UK;
[f] Vascular Biology Program, Boston Children's Hospital, Harvard Medical School, Boston, MA 02115 ;
[g] Department of Molecular and Translational Medicine, University of Brescia, Brescia, Italy;
[h] Department of Mechanical and Industrial Engineering, National Interuniversity Consortium of Materials Science and Technology, University of Brescia, Brescia, Italy;
[i] Consorzio Interuniversitario per lo Sviluppo dei Sistemi a Grande Interfase, Florence, Italy;
[j] National Research Council, Institute of Nanostructured Materials, Bologna, Italy;
[k] Department of Chemistry, University of Florence, Florence, Italy;
[l] Center for Excellence in Vascular Biology, Cardiovascular Medicine, Brigham and Women's Hospital, Harvard Medical School, Boston, MA 02115;
[m] Institute for Research and Biomedical Innovation, National Research Council, Palermo, Italy

[#] To whom correspondence may be addressed. Email: weinbaum@ccny.cuny.edu or eaikawa@bwh.harvard.edu.

**This PDF file includes:**

## Supplemental Materials and Methods

### Cell culture and isolation of extracellular vesicles

Human coronary artery smooth muscle cells (SMCs; PromoCell) were expanded, plated for extracellular vesicle (EV) isolation and grown to confluence using 'Smooth Muscle Cell Growth Medium 2' (5% v/v serum; PromoCell). Cells were then cultured in either control, 'normal' medium of Dulbecco's Modified Eagle Medium (DMEM) plus 10% fetal bovine serum (FBS) and 1% penicillin/streptomycin, or calcifying, 'osteogenic' medium comprised of control medium plus 10 nM dexamethasone, 100 μM L-ascorbic acid and 10 mM β-glycerophosphate. The media were exchanged every 48 to 72 hours. After at least 14 days of culture (sufficient time to induce osteogenic differentiation of the SMCs (1)), the media were exchanged for control or calcifying medium of only 0.1% FBS, to minimize the presence of FBS-derived vesicles in the media. After 24 hours the conditioned 0.1% FBS media were collected, centrifuged for 10 minutes at 1,000*g*, and EV-containing supernatants were stored at -80 $^{o}$C. For vesicle experiments, EVs were washed using centrifugal filtration (Millipore Amicon Ultra Centrifugal Filter Unit with membrane nominal molecular weight limit of 3 KDa) and concentrated using the same centrifugal filtration equipment. The final vesicle suspension volume was adjusted to achieve a vesicle concentration four-times that of the original vesicle concentration in conditioned media (e.g., if starting with 8 mL, the final volume was 2 mL).

### EV assay for calcification potential

An assay for alkaline phosphatase activity, a key regulatory enzyme of vascular calcification (2), was used to determine the calcification potential of SMC-isolated EVs (AnaSpec SensoLyte® pNPP Alkaline Phosphatatse Assay Kit). Briefly, EVs contained within 1ml of isolated supernatant were pelleted using ultracentrifugation at 100,000*g* for 40 minutes, and resuspended in a solution of 0.2% Triton® X-100 in the provided assay buffer. Resultant values were normalized against protein content (Thermo Scientific Pierce™ BCA Protein Assay Kit).

### Nanoparticle-tracking analyses (NTA)

NanoSight LM10 (Malvern Instruments) was used to conduct NTA of EV size and concentration within the baseline media isolates and following experiments investigating EV aggregation and calcification in suspension. Vesicles were diluted 1:7 in phosphate buffered saline (PBS) and injected into the laser-illuminated NanoSight chamber. If the vesicle suspension was 4x concentrated during experiment set-up, then the suspension was diluted 1:28. The diluted sample was continuously injected into the chamber using a syringe pump (Malvern), during which five NTA movies were collected, each 1-minute in duration. The distribution of nanoparticle size and concentration within the sample is determined by an analysis of the Brownian motion of the

objects recorded in the NTA movies (3). The camera gain used was 9 and the vesicle detection threshold value used was 2. The size and concentration analyses from each movie were averaged, yielding a representative set of data for each sample.

**EV aggregation and calcification in suspension**

Calcifying EVs were concentrated 4x (as above) and incubated in eppendorf tubes, 400ul per tube, for 8 days at 37$^{o}$C. At the assigned time points, 57.1 µL of 0.4 mM ibandronate (Sigma-Aldrich) or water (untreated control) was added to the appropriate tubes. The effect of BiP on tissue non-specific alkaline phosphatase (ALP) activity was measured by adding ibandronate or water to suspensions of EVs at the concentrations listed above, and measuring ALP activity at baseline or following 1,2 or 4 hours of incubation, using the assay described in the "EV assay for calcification potential" section above.

**EV mineralization assay**

The mineralization of EVs incubated in suspension was quantified using a fluorescent-based mineral-binding dye (Lonza, OsteoImage). Briefly, EV suspensions were ultracentrifuged (100,000*g*, 40 minutes, 4 $^{o}$C), the pellet was resuspended in 200 µL of OsteoImage dye and incubated for 30 minutes at room temperature. Using ultracentrifugation, the dye was removed, and the pellets were washed twice with OsteoImage wash buffer. The final pellet was resuspended in 100 µL of OsteoImage wash buffer and fluorescent intensity was recorded using a plate reader. Data for Fig. 5*B* was normalized using the average of the 'no treatment' group for each biological replicate, (n=5 biological replicates).

**3D collagen hydrogel experiments**

Collagen hydrogels were cast onto amino-silanated, round (neuVitro, 12mm diameter), glass coverslips, following an adaptation of a previously established protocol (4). Briefly, 150 µL of 0.1M NaOH was added to each coverslip, which was then heated on a hotplate at 80 $^{o}$C until the liquid evaporated. The coverslips were removed from the hotplate and 6 drops of (3-aminopropyl) triethoxysilane (APES) was added to the NaOH-treated surface for 5 minutes, then rinsed off under a stream of DI water. The coverslips were transferred to individual wells of a 24 well-plate, treated side up, washed twice with DI water, 5 minutes per wash, then covered with 0.5% glutaraldehyde in PBS for 30 minutes at room temperature. The coverslips were removed from the glutaraldehyde solution, allowed to air-dry and then UV sterilized in a cell culture hood for 30 minutes.

The sterile, amino-silanated coverslips were immediately covered with 75 µL of a 5% solution of rat tail high concentration collagen type I (Corning) in 0.1% FBS calcifying medium, pH 7-8, gels set for 1 hour at 37 $^{o}$C. Calcifying EVs were added, 400 µL per gel, and incubated at 37 $^{o}$C for 8

days. At the indicated time points, 57.1 µL of water (untreated control) or 0.4 mM ibandronate in water (Sigma-Aldrich) was added, final ibandronate concentration 0.05 mM. At the end of each experiment, the coverslip-adhered hydrogels were further processed for imaging, as described below.

**Scanning electron microscopy (SEM) and elemental analysis**

Following incubation with calcifying EVs, coverslip-adhered collagen hydrogels were immersed in 2% gluataraldehyde in 0.1M sodium cacodylate buffer, pH 7.2, for 1 hour. The fixed hydrogels were rinsed three times in 0.1M sodium cacodylate buffer, pH 7.2, 15 minutes per rinse. The hydrogels were then dehydrated in grades of ethanol (10min each; 35%, 50%, 70%, 80%, 95%, 100% x3).

The dehydrated collagen gels were then subjected to critical point drying (Tousimis 931 GL), mounted onto aluminum stubs (Electron Microscopy Sciences, EMS) using 12mm diameter carbon adhesive tabs (EMS), and sputter coated (EMS 300T D Dual Head sputter coater) with 5 nm of 80:20 platinum:palladium. The uncoated edges of each sample were covered with silver adhesive (EMS). Samples were imaged in a Supra55VP FESEM (Zeiss) using a secondary electron in-lens detector, 6.4 mm working-distance, and 8.00 kV beam voltage. An energy-dispersive x-ray spectroscopy (ED) detector was used to perform elemental analysis, beam energy 8 kV.

**Quantification of microcalcification area**

An algorithm was custom-written (MATLAB) to calculate the average area of the five largest microcalcifications per high-powered field (2k magnification) imaged using SEM. Each image was converted from grayscale to binary using a >10% luminance threshold. Microcalcifications were then defined using serial image processing filters, first filtering for adjacent pixels with minor axis length of 2.5 to infinity, then unconnected pixels were bridged together, then for an area of 75 to infinity, then for a minor axis length of 5 to infinity. Then, identified objects with an eccentricity >95% and an area <150 were filtered out, as these objects were noise within the data. Finally, the average area of the five largest objects was calculated for each image (n=13 for the control group and n=13 for the treatment group, three biological replicates represented in each).

**Measuring geometric characteristics of individual microcalcifications**

Characteristics of individual microcalcifications (circularity and area) were measured using ImageJ (NIH). For each SEM image of a single microcalcification, the microcalcification was outlined by hand and a mask was created from the outline. The ‘analyze particles’ function was then used, which measured the circularity and area (in pixels squared) of the mask. The area was

converted to micrometers squared based on measurements of the scale bar included in each SEM image.

**Transmission Electron Microscopy (TEM)**

Collagen hydrogels for TEM were prepared as described above but cast in chambered coverglass wells (LAB-TEK, no. 1.5 borosilicate), 300 µL per well. Calcifying EVs were concentrated 7.5x and added to each gel, along with a suspension of ibandronate or water, such that the total volume added per gel was 250 µL and the final concentration of ibandronate was 0.05 mM. Samples were fixed for 2 hours at room temperature with 2.5% glutaraldehyde/2% paraformaldehyde in 0.1 M sodium cacodylate buffer, pH 7.4. The samples were washed in 0.1 M cacodylate buffer and postfixed with 1% osmiumtetroxide (OsO4)/1.5% potassiumferrocyanide ($KFeCN_6$) for 1 hour, washed in water 3x and incubated in 1% aqueous uranyl acetate for 1 hour followed by 2 washes in water and subsequent dehydration in grades of alcohol (10 minutes each: 50%, 70%, 90%, 100%, 100%). The samples were then put in propyleneoxide for 1 hour and infiltrated overnight in a 1:1 mixture of propyleneoxide and TAAB Epon (Marivac Canada Inc. St. Laurent, Canada). The following day the samples were embedded in TAAB Epon and polymerized at 60 $^{o}$C for 48 hours.

Ultrathin sections (~ 80 nm) were cut on a Reichert Ultracut-S microtome, picked up on to copper grids stained with lead citrate and examined in a JEOL 1200EX Transmission electron microscope, images were recorded with an AMT 2k CCD camera.

**Fourier-transform infrared spectroscopy (FTIR)**

Fourier transform infrared spectroscopy (Bruker, FTIR) was used to perform chemical analyses of microcalcifications. For this experiment, vesicles were washed using centrifugal filtration as detailed in the ‘cell culture and isolation of extracellular vesicles’ section, but the final vesicle suspension volume was equal to the starting volume, achieving a 1x vesicle concentration as opposed to the 4x concentration used in other experiments. Vesicles were otherwise then prepared and incubated as detailed in the ‘EV aggregation and calcification in suspension’ section. Samples were then ultracentrifuged (100,000*g*, 40 minutes, 4 $^{o}$C), the pellet resuspended in 50 µL of PBS, and dropcast onto an untreated glass slide. A motorized stage and polarized optical microscope was used to identify regions for analysis. Attenuated total reflectance mode (single bounce Ge crystal) was used to collect spectral data in a range from 4,000 to 600 $cm^{-1}$. Each spectrum was normalized by dividing each data point by the sum of the values from 2,000 to 700 $cm^{-1}$.

**Confocal microscopy**

Confocal microscopy was used to quantify the size of microcalcifications formed in the 3D

collagen hydrogel experiments. One day before sample collection and imaging, (day 7), a near-infrared calcium tracer (OsteoSense 680, Perkin Elmer) was added to each hydrogel-containing well and incubated at 37 ºC. The following day, coverslip-adhered hydrogels were mounted onto glass slides using SHUR/*Mount*™ (TBS). Gels were imaged using continuous-wave confocal microscopy (Nikon A1), 8 sets of z-stack optical sections were collected per gel, each stack encompassing the entire fluorescent signal present within that region of the gel.

**Multiscale Finite Element Analysis (FEA)**

Multiscale finite element analysis was computed in ABAQUS (version 6.14.3, Simulia, Providence, RI). A global finite element (FE) model and three submodels were prepared to obtain the stress concentration factor (SCF) produced by the presence of a single microcalcification. For the global model, a 3D FE volumetric tetrahedral mesh was created, depicting the soft tissue, lipid and cap of the atheroma. Material properties were assigned using an incompressible neo-Hookean isotropic hyperelastic model, strain energy function $W = C(I1 - 3)$, C is a material constant, initial Young's modulus $E = 6 \times C$, and I1 is the first invariant of the strain tensor. 120 mmHg were applied as hydrostatic load on the lumen of the artery and stresses and strains were recorded at each node. The first-level submodel consisted of the whole cap, with results from the global model driving the boundary conditions and much smaller size finite elements. The second-level submodel consisted of a segment of the cap, in which the size of the finite elements were again reduced to increase accuracy. In the third-level submodel, a smaller region of interest of the cap, 20x20x20 μm, was prepared, in which the SEM-based microcalcifications were included. The material properties of the cap remained the same, but the regions corresponding to the microcalcifications from SEM were assigned linear elastic material properties corresponding to calcified tissue (10GPa). Boundary conditions were driven by results from the second submodel. 3D maps of stresses and strains were obtained for each SEM-imaged microcalcification. Control tests were performed by assigning soft tissue, hyperelastic properties to the 3D volume occupied by the microcalcifications stress concentration was calculated as the ratio of the stresses with and without microcalcifications and measured for three distinct microcalcifications per treatment group.

**Atomic Force Microscopy (AFM)**

*Sample preparation and imaging* - EVs were concentrated 4x and incubated in suspension and treated with ibandronate as above. Following 8 days of incubation, samples underwent ultracentrifugation, and the pellets were frozen and shipped on dry ice to the co-authors in Italy. The pellets were thawed and resuspended in 100 μL sterile MilliQ water added with protease inhibitor 1:1000. 4-6 μL of sample were then spotted onto freshly cleaved mica sheets (Grade V-1, thickness 0.15 mm, size 15x15 $mm^2$), incubated at 30°C for 20 minutes over a heating plate to

let the sample droplet dry. Images were acquired with a NaioAFM (Nanosurf AG) equipped with Multi75Al-G probe (Budget Sensors, Sofia, Bulgaria) in tapping mode, scan size ranging 2 µm to 25 µm, scan speed 0.8 s to 1.0 s per scanning line. Imaging analysis was performed with the software WSxM 5.0 image (5), using 5 µm x 5 µm images.

*Indentation of calcifying EV samples* - 4-6 µl of calcifying EV samples were deposited onto freshly cleaved mica sheets and dried as above. The samples were imaged to localize EVs and microcalcifications, using a NaioAFM (Nanosurf AG) equipped with ContAl-G probe (nominal spring constant k ~ 0.2 N▪m-1 Budget Sensors, Sofia, Bulgaria), in contact mode, scan size 20 µm to 5 µm, scan speed 1.0 s per scanning line. The AFM probe was then positioned above the center of each EV/microcalcification, and individual force curves were recorded with a Z-starting offset of 500 nm and a Z-piezo speed of XYZ 10 µm▪$s^{-1}$. The force distance curves were then analyzed with the software SPIP 6.7.2 (Image Metrology A/S, Denmark).

**Human carotid endarterectomy tissue**

Human carotid artery samples were obtained from patients undergoing endarterectomy (Brigham and Women's Hospital Institutional Review Board protocol #1999P001348). The IRB approved a waiver of informed consent and authorization for the use of excess human material from clinical procedures that would otherwise be discarded, in compliance with federal regulation 45 CFR 46.116., the demographic and clinical information of donors is not available.

**Animal study – atherogenic mouse model receiving bisphosphonate treatment**

The in vivo study was performed using procedures approved by the Institutional Animal Care and Use Committee (IACUC) at Florida International University. Eight-week-old mice homozygous for the Apoetm1Unc mutation (B6.129P2-Apoetm1Unc/J, ApoE-/-) were purchased from Jackson Laboratory (Bar Harbor, ME). After two weeks of incubation and feeding with chow diet, n = 16 animals (10 weeks old) received an atherogenic diet (ENVIGO, TD.88137 adjusted calories diet 42% from fat) for 25 weeks. Multiple prior studies have demonstrated the early formation of microcalcifications in $ApoE^{-/-}$ and $LDLR^{-/-}$ mice fed for 10-24 weeks (2-<6 months) with an atherogenic diet starting at 8-10 weeks of age (6–10). These prior studies visualized and quantified vascular microcalcification formation utilizing various techniques, ranging from more traditional Alizarin Red S or von Kossa staining (7, 9) to the targeted fluorescent probe OsteoSense680 (a bisphosphonate-derived near-infrared fluorescent imaging probe), imaged using both intravital microscopy and near-infrared fluorescence imaging (6–9, 11). In these studies, OsteoSense680 staining demonstrated microcalcification formation as early as after 10 weeks of diet (6, 7), and more extensive microcalcification formation after 15-20 weeks of diet (6–10).

The animals were sorted into four groups, n = 4 animals per group. Three groups received twice weekly subcutaneous injections of bisphosphonate ibandronate sodium (2 mg/kg mouse per dose, APEXBIO) after 5, 10, and 15 weeks of diet, respectively. Specifically, BiP was given after 5 weeks of diet, before the expected onset of microcalcification ('Week 5 BiP'), after 10 weeks of diet, the expected time of initial microcalcification formation ('Week 10 BiP'), or after 15 weeks of diet, once microcalcification formation has been established ('Week 15 BiP'). The fourth group, control, was injected twice weekly with the reagent vehicle, PBS (1X). After 25 weeks, the mice were sacrificed, and the aortas were resected and fixed in formalin solution (10% phosphate buffer, Fisher scientific) for 24 hours. The tissues were embedded using optimal cutting temperature compound (Tissue-Plus, Fisher Healthcare) through a slow freezing process. To assess mineral morphology in the atherosclerotic plaques, 18 μm thick histological sections were prepared for SEM from the embedded tissues. Representative histological images demonstrating positive Alizarin Red S staining and corresponding H&E images for representative mouse aortic tissue samples from all experimental groups following 25 weeks (6 months) of atherogenic diet are provided in Fig. S8 and S9. Alizarin Red S staining was performed because this dye binds specifically to calcium and therefore, is a more sensitive marker of microcalcification deposition, while H&E staining is known to underestimate microcalcification deposition (6).

**Histological Analyses**

The embedded tissues were sectioned with the thickness of 18 μm and placed on microscope glass slides (EMS). After the removal of the OCT using DI water, the cryosections were incubated with 1% w/v Alizarin Red S staining (RICCA) at room temperature for 5 minutes. The sections then were rinsed three times with DI water, treated with xylene (Sigma), and mounted for imaging. For Hematoxylin and Eosin (H&E) staining, the OCT was removed with ethyl alcohol (Sigma), and the cryosections were stained with Hematoxylin stain solution (RICCA) and Eosin-Y stain (Fisher HealthCare) according to the protocols. The images were taken using an inverted microscope (Zeiss, Axiovert 40 CFL).

**Quantitative analysis of *in vivo* calcification size and roughness**

To assess the average of the mineral surface roughness (Ra) and the average area of microcalcifications imaged from histologic samples via DDC-SEM, a custom image analysis script was developed in MATLAB. Briefly, after filtering the background (organic material) from the image, individual microcalcifications were identified as connected pixels in binarized images. Ra was determined as the mean deviation from the average grayscale intensity in each microcalcification as performed previously (12–14). A higher Ra indicates more deviation in signal intensity, which corresponds to a more heterogenous (i.e., rougher) surface. The area of each microcalcification

was also measured. The Ra and area values were then averaged across images for each mouse, and the data reported represent the mean values calculated from different mice, n = 3 biological replicates per group.

**Statistical analyses**

Error bars represent standard deviation, unless stated otherwise. Quantitative data was analyzed for statistical significance using a Student's T-test (Microsoft Excel) if comparing two groups. When comparing multiple groups, a one-way ANOVA was used with either Tukey's Multiple Comparisons Test (Fig. 6*I,J*, Fig.7*E*, Fig. 8*B-C*) or Dunnett's Multiple Comparisons Test (Fig. 5*B*) if equal variability of differences was not assumed (GraphPad Prism). For Figures S5 and S6, a two-way comparison between multiple variables was performed, using a two-way ANOVA (Fig. S5) or mixed effects model (Fig. S6) with the Geisser-Greenhouse correction in both instances (GraphPad Prism). Significance was defined as $p < 0.05$.

The statistics for Figure S7 are an exception, the error bars represent a normalized error value, accounting for error propagation using classical error theory. One representative sample was used for analysis of each control/treatment group represented in Figure S7. For each sample, the detachment force for the mica substrate was measured at multiple points, and the average detachment force ($F_{substrate}$) and standard error was calculated. Then, for each sample, several individual EVs or microcalcifications were identified and the detachment force was measured for each. The average detachment force ($F_{calcification}$) and standard error was calculated. The normalized detachment force for each sample was calculated as ($F_{calcification}$) / ($F_{substrate}$). The normalized error was calculated using the propagation of uncertainty through a quotient.

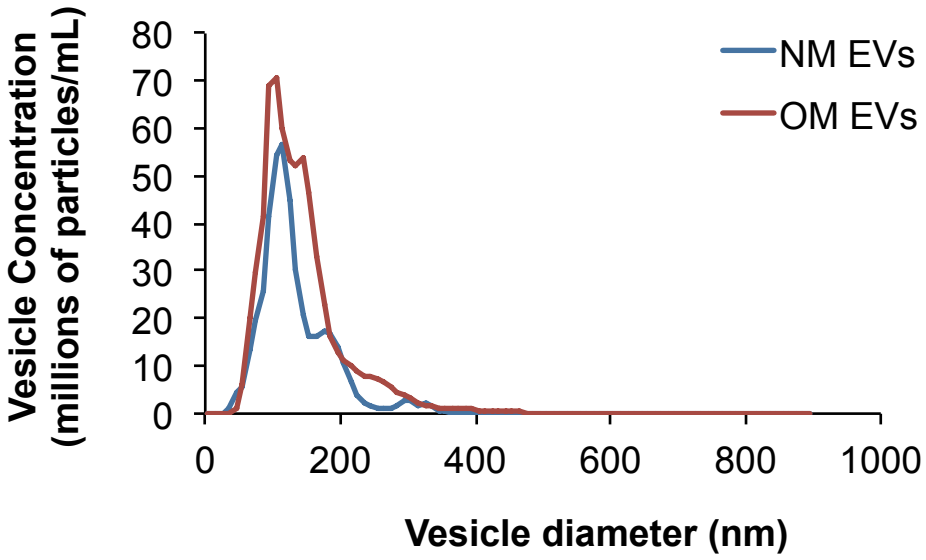


**Fig. S1.** Baseline size distribution of EVs isolated from vSMCs cultured in normal medium (NM, blue) or osteogenic medium (OM, red). Measurements were performed using nanoparticle tracking analysis (NTA), 5 NTA runs per group, n = 1 biological replicate.

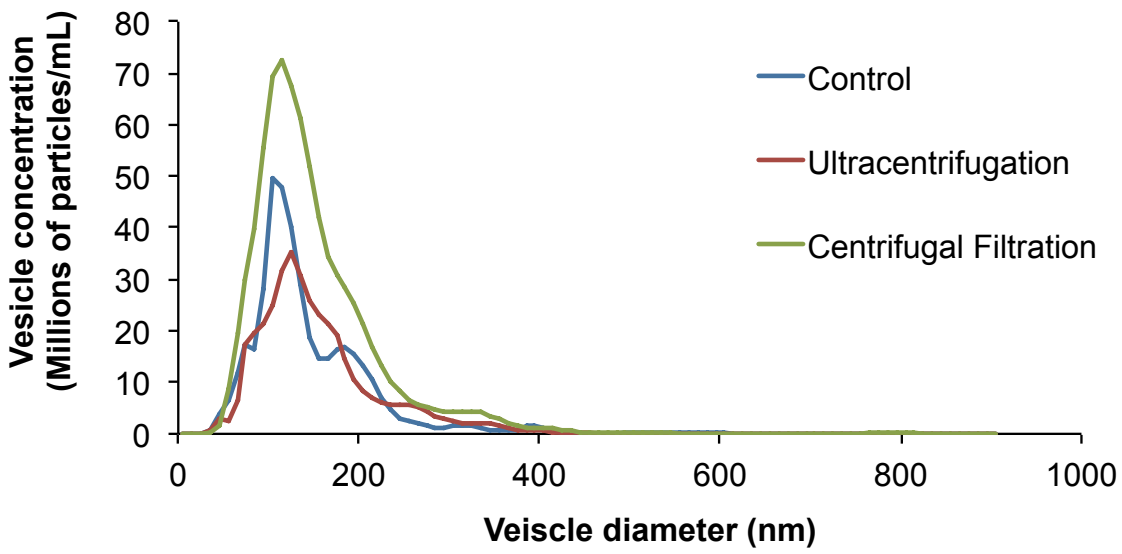


**Fig. S2.** Baseline size distribution of EVs isolated from vSMCs cultured in osteogenic medium, that were subsequently washed using ultracentrifugation (red), centrifugal filtration (green) or unwashed (blue). Measurements were performed using nanoparticle tracking analysis (NTA), 5 NTA runs per group, n = 1 biological replicate.

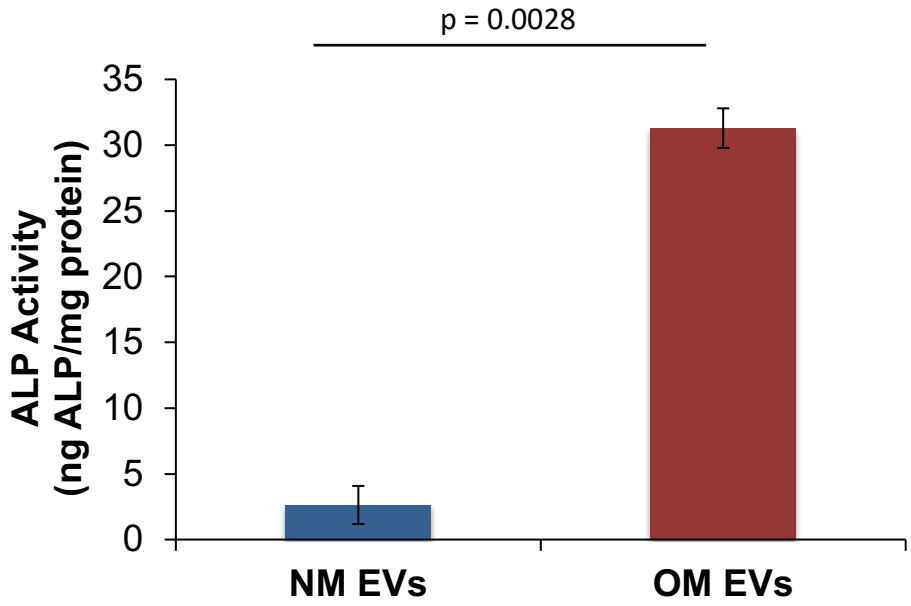


**Fig. S3.** Representative tissue non-specific alkaline phosphatase (ALP) activity of EVs isolated from vSMCs cultured in normal medium (NM) or osteogenic medium (OM), for 17-19 days. n = 3 biological replicates, p-value determined by two-tailed Student's T-test

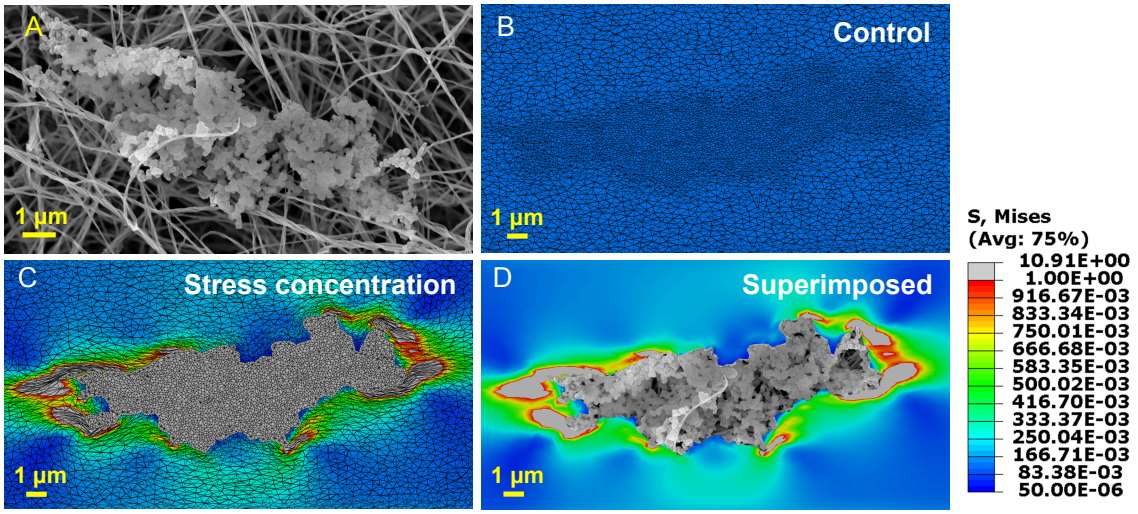


**Fig. S4.** Multiscale finite element analysis (FEA) was used to predict the in vivo tissue stress that would be associated with the microcalcifications formed in our in vitro 3D platform. A SEM image of a representative microcalcification formed in the platform was selected (A) and virtually inserted into the fibrous cap of the simulated atheroma. To conduct a baseline calculation, the microcalcification structure was first assigned 'soft' material properties equivalent to the fibrous cap, and FEA predicted a negligible increase in fibrous cap tensile stress (B– blue color). However, when the microcalcification structure was assigned 'hard' material properties of mineral, FEA predicted a 350% increase in fibrous cap tensile stress (stress concentration factor, or SCF) due to the presence of this single microcalcification (C and D– red color).

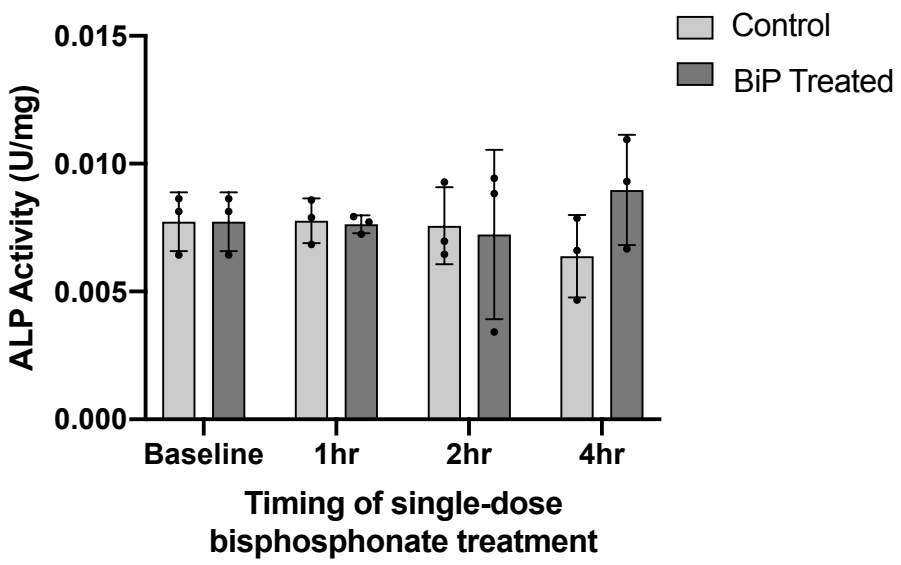


**Fig. S5.** Tissue non-specific alkaline phosphatase (ALP) activity in EVs suspended in osteogenic media following treatment with BiP at t=0 versus untreated control. No difference between treatment groups at any time point, p=0.53 via two-way ANOVA (n=3 biological replicates)

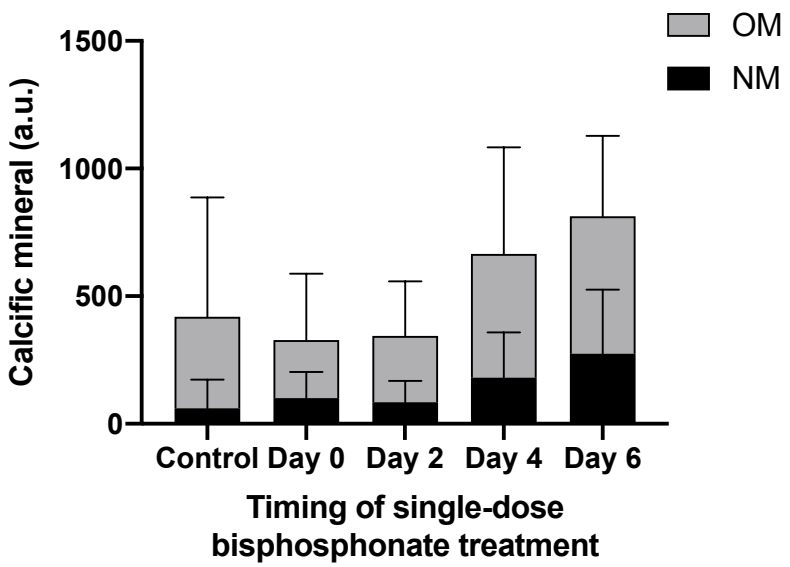


**Fig. S6.** Calcific mineral was measured following single-dose BiP treatment of EV in suspension in either osteogenic media (OM) or normal media (NM), with a significantly higher degree of calcification in osteogenic medium, p=0.028, via mixed effects model (n=4 biological replicates).

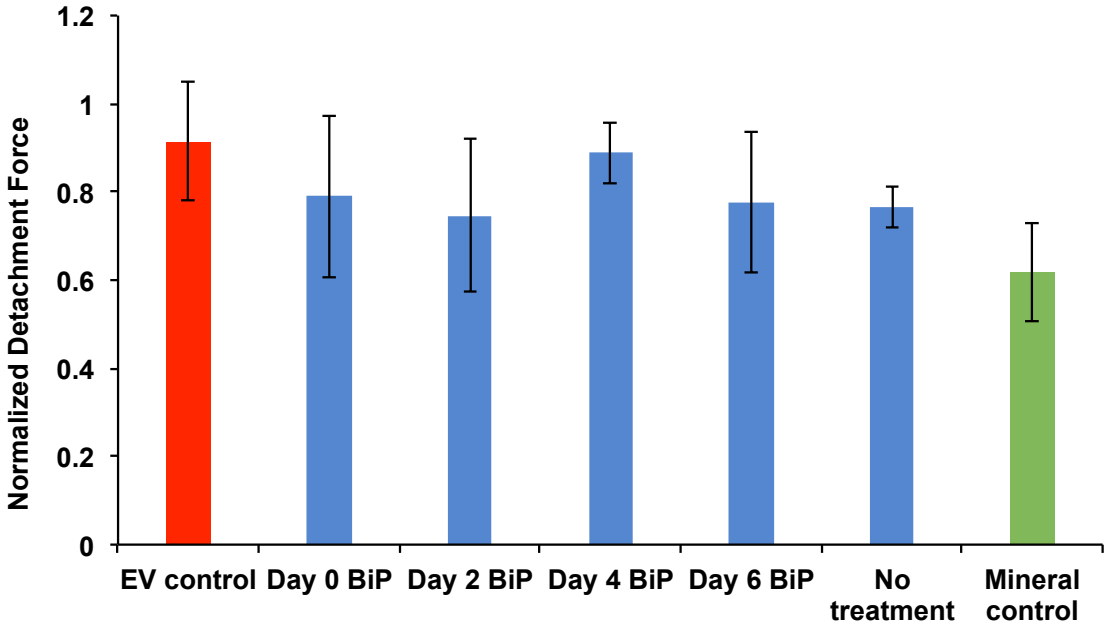


**Fig. S7.** Normalized detachment force of BiP-treated and untreated microcalcifications (blue bars) fell between that for isolated EVs (red bar) or isolated calcium phosphate mineral (green bar).

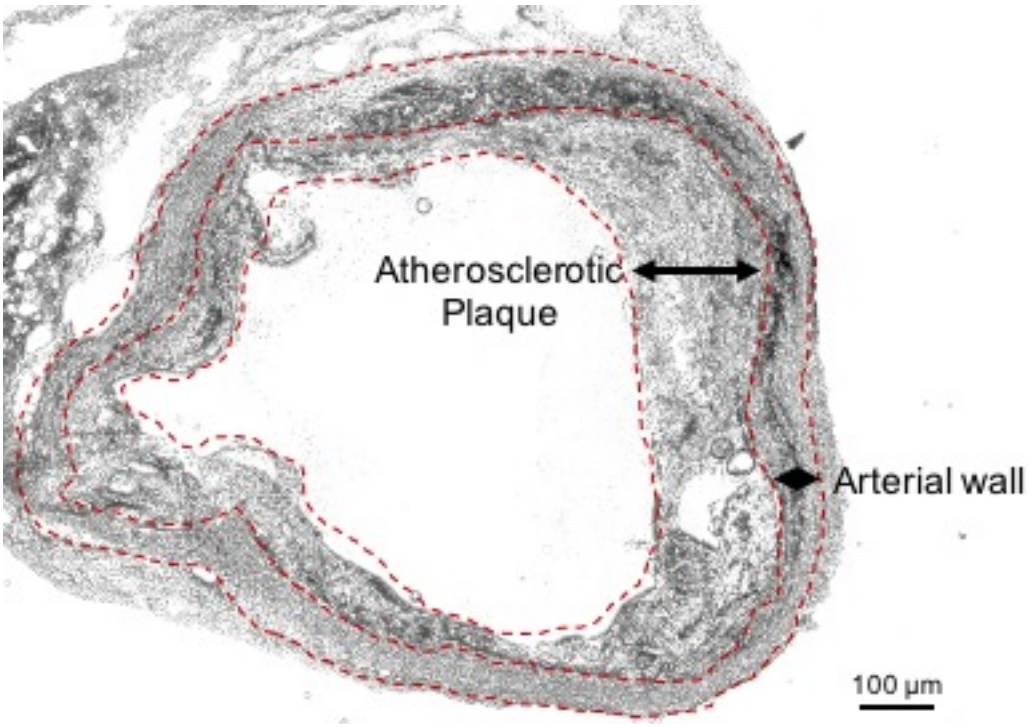


**Fig. S8.**
Representative brightfield microscopy image of the aortic root of a 35-week-old Apoe$^{-/-}$ mouse in the control group, following 25 weeks of atherogenic diet, demonstrating the occurrence of atherosclerosis in these mice.

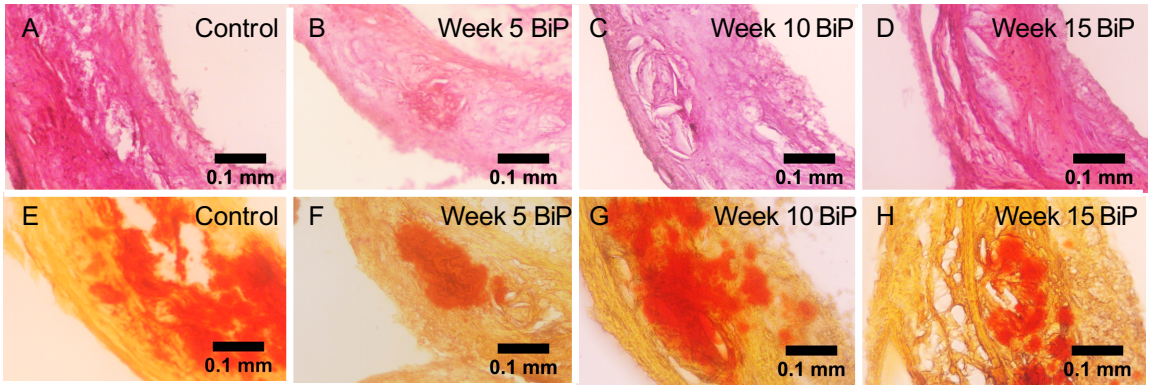


**Fig. S9.**
Representative histological H&E staining (A-D) and Alizarin Red S staining demonstrating calcification (E-F, red-stained areas) of mouse aorta from in vivo experiment depicted in Fig. 8, following 25 weeks of atherogenic diet. Panels A, E represent mice from the control group. Panels B, F represent mice treated with BiP following 5 weeks of diet. Panels C, G represent mice treated with BiP following 10 weeks of diet. Panels D, H represent mice treated with BiP following 15 weeks of diet. Scale bar = 0.1mm in all images.

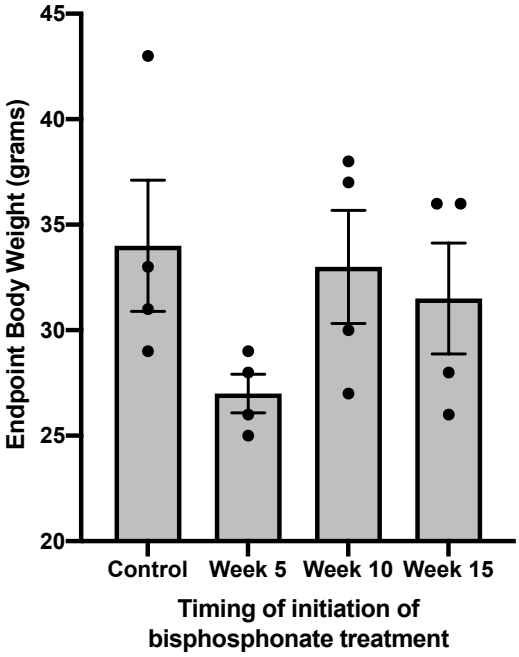


**Fig. S10.** Average body weight for the mice in each experimental group following 25 weeks of diet, n = 4 mice per group, error bars represent standard deviation. There was no significant difference between the groups calculated by one-way ANOVA, p = 0.25

**SI References**


1. Steitz SA, et al. (2001) Smooth muscle cell phenotypic transition associated with calcification: Upregulation of Cbfa1 and downregulation of smooth muscle lineage markers. *Circ Res* 89(12):1147–1154.
2. Hutcheson JD, et al. Enrichment of calcifying extracellular vesicles using density-based ultracentrifugation protocol. doi:10.3402/jev.v3.25129.
3. Wright M (2012) Nanoparticle tracking analysis for the multiparameter characterization and counting of nanoparticle suspensions. *Methods Mol Biol* 906:511–24.
4. Tse JR, Engler AJ (2010) Preparation of hydrogel substrates with tunable mechanical properties. *Curr Protoc Cell Biol* (SUPPL. 47):1–16.
5. Horcas I, et al. (2007) WSXM: a software for scanning probe microscopy and a tool for nanotechnology. *Rev Sci Instrum* 78(1):013705.
6. Aikawa E, et al. (2007) Osteogenesis associates with inflammation in early-stage atherosclerosis evaluated by molecular imaging in vivo. *Circulation* 116(24):2841–2850.
7. Hutcheson JD, et al. (2016) Genesis and growth of extracellular-vesicle-derived microcalcification in atherosclerotic plaques. *Nat Mater* 15(3):335–43.
8. Goettsch C, et al. (2016) Sortilin mediates vascular calcification via its recruitment into extracellular vesicles. *J Clin Invest* 126(4):1323–1336.
9. Derwall M, et al. (2012) Inhibition of bone morphogenetic protein signaling reduces vascular calcification and atherosclerosis. *Arterioscler Thromb Vasc Biol* 32(3):613–622.
10. Yao Y, et al. (2010) Inhibition of bone morphogenetic proteins protects against atherosclerosis and vascular calcification. *Circ Res* 107(4):485–494.
11. Okui T, et al. (2020) CROT (Carnitine O-Octanoyltransferase) Is a Novel Contributing Factor in Vascular Calcification via Promoting Fatty Acid Metabolism and Mitochondrial Dysfunction. *Arterioscler Thromb Vasc Biol*:ATVBAHA120315007.
12. Samtaş G (2014) Measurement and evaluation of surface roughness based on optic system using image processing and artificial neural network. *Int J Adv Manuf Technol* 73(1):353–364.
13. Kamguem R, Tahan SA, Songmene V (2013) Evaluation of machined part surface roughness using image texture gradient factor. *Int J Precis Eng Manuf* 14(2):183–190.
14. Alshibli KA, Druckrey AM, Al-Raoush RI, Weiskittel T, Lavrik N V. (2015) Quantifying Morphology of Sands Using 3D Imaging. *J Mater Civ Eng* 27(10):04014275.